The Eleventh International Conference on
Engineering Computational Technology
23–25 August, 2022 | Montpellier, France

Proceedings of the Eleventh International Conference on
Engineering Computational Technology
Edited by B.H.V. Topping and P. Iványi
Civil-Comp Conferences, Volume 2, Paper 1.3
Civil-Comp Press, Edinburgh, United Kingdom, 2022, doi: 10.4203/ccc.2.1.3

Parallel adaptive simulation of rotating detonation engines

H. Peng and R. Deiterding

Aerodynamics and Flight Mechanics Research Group
University of Southampton, United Kingdom

Abstract

The rotating detonation engine is a promising realization of pressure gain combustion for propulsion and power generation systems. A rotating detonation engine running on ethylene-oxygen is simulated by using AMROC with a second-order accurate finite volume method and approximate Riemann solvers. Multi-step chemical kinetic mechanisms are employed with a splitting approach. The rotating detonation is studied in a 2-D unwrapped chamber with premixed and non-premixed injections and is then simulated in a 3-D annular chamber. The results show that using the adaptive mesh refinement method can simulate rotating detonation problems efficiently.

Keywords: rotating detonation engine, reactive flow simulation, adaptive mesh refinement, adaptive curvilinear mesh, parallelization.

1 Introduction

The rotating detonation engine (RDE), which employs pressure-gain combustion, is presently being considered as a particularly promising combustion chamber replacement for power and propulsion systems [1]. In an RDE, one or multiple detonation waves propagate rapidly in the combustor, resulting in a nearly constant-volume combustion process that produces high-pressure burnt products and can provide thrust directly. The visualisation of the internal flow field in RDEs experiments is challenging since the detonation wave travels in an RDE at high temperature, high pressure, and high speed. Computational fluid dynamics (CFD) research provides an approach to studying the complex flow in RDEs [2].

Most of the simulations on RDEs were conducted using premixed injections and based on a simplified one- or two-step chemical model [3, 4]. Yet, in realistic experimental tests, the premixed propellants may cause a backfire into the plenum if no specialised injectors are employed. It is hence necessary to conduct some simulations based on non-premixed injection [5]. A multi-step chemical model is also required to improve the flexibility and accuracy when simulating a non-premixed process in RDEs [6].

In order to understand the detonation propagation process and the internal flow structure of RDEs, a high-resolution simulation with a detailed chemistry mechanism should be used. The extreme thermodynamic conditions in RDEs make simulations costly and challenging. An effective approach for simulating detonation problems is adaptive mesh refinement (AMR). The grids are refined dynamically in the regions where the physical variables change dramatically [7].

In the present work, simulations are based on our parallel block-structured mesh adaptation framework AMROC (Adaptive Mesh Refinement in Object-oriented C++) [8]. An annular RDE is simulated with a 2-D unwrapped model on Cartesian adaptive meshes. Premixed and non-premixed ethylene/oxygen mixtures are injected through discrete slots. The effects of the non-uniform local equivalence ratio on rotating detonation waves are studied. Then a three-dimensional computation is carried out by using a recently developed solver [9] in AMROC based on curvilinear adaptive meshes.

2 Methods

The multi-species compressible Euler equations with a detailed chemical model are solved as governing equations:

$$\begin{aligned} &\partial_t(\rho \boldsymbol{Y}) + \nabla\cdot(\rho \boldsymbol{u} \boldsymbol{Y}) = \dot{\omega} \\ &\partial_t(\rho \boldsymbol{u}) + \nabla\cdot(\rho \boldsymbol{u}\boldsymbol{u} + p\boldsymbol{I}) = 0 \\ &\partial_t(\rho E) + \nabla\cdot(\rho \boldsymbol{u}(E + p/\rho)) = 0 \end{aligned} \tag{1}$$

The total specific energy can be computed through the temperature- and species-dependent enthalpy and specific heat ratio. The multi-species ideal gas state equation is used to close the system. The mass generation rate of each component can be calculated by a chemical reaction mechanism of multiple steps as:

$$\dot{\omega}_i = \sum_{j=1}^{J}\left(\nu_{ji}^r - \nu_{ji}^f\right)\left[k_j^f \prod_{n=1}^{N_{sp}}\left(\frac{\rho_n}{W_n}\right)^{\nu_{jn}^f} - k_j^r \prod_{n=1}^{N_{sp}}\left(\frac{\rho_n}{W_n}\right)^{\nu_{jn}^r}\right], \quad i = 1,\ldots N_{sp} \tag{2}$$

The rate constant of the chemical reaction is given by the Arrhenius formula:

$$k_j^{f/r}(T) = A_j^{f/r} T^{\beta_j^{f/r}} exp\left(-\frac{E_j^{f/r}}{RT}\right) \tag{3}$$

The inviscid fluxes are evaluated by a hybrid Roe/HLL scheme [8] or a HLLC scheme with pressure-based wave estimates [10]. The dimensional splitting method is used to deal with the multi-dimensional problems. A second-order accurate MUSCL-Hancock scheme with Minmod limiter is used for the reconstruction. A

reduced ethylene-oxygen mechanism with 10 species and 10 reactions [11] is employed. Strang splitting is adopted for integrating the reactive source term. For the 3-D solver, the coordinates of a uniform Cartesian mesh in computational space are firstly mapped onto the coordinates of a non-uniform, curvilinear structured mesh in physical space by a cylindrical mapping function. A cell-centred finite volume method is used to discretise the multi-component Euler equations in physical space. The capacity function approach [12] is employed and facet-dependent rotation matrices are used to rotate the velocities aligning with the grid. A conservative averaging is used for the fine-to-coarse restriction. A trilinear interpolation is applied for the coarse-to-fine gird prolongation, which involves a local nonlinear system solved by a Newton-Raphson method. If this method is not convergent within given iteration steps, the gradient descent algorithm would be used.

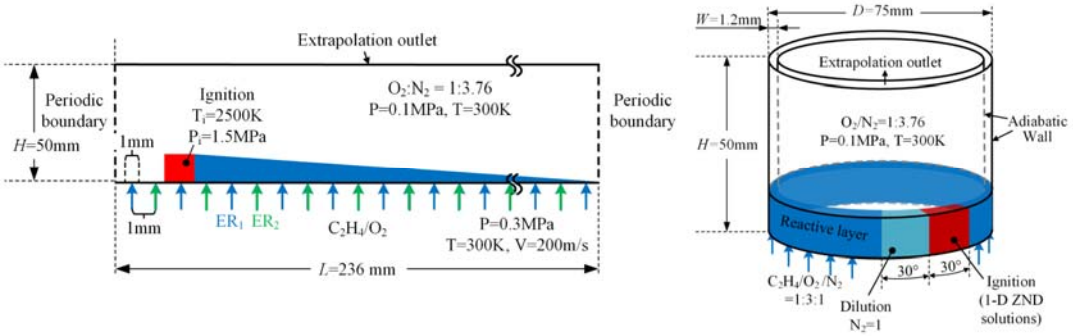

Figure 1: 2-D and 3-D computational domain of the RDE simulations.

The computational domains of the 2-D unwrapped and 3-D annular RDEs are shown in Figure 1, which is referring to an actual micro RDE laboratory experiment [13]. The initial condition and boundary conditions are also given in this figure.

3 Results

The base grid in the 2-D calculations is 0.25 mm. The maximal refinement level is set to 4 with a uniform refinement factor of 2 on each level. The respective minimum mesh size is 0.03125 mm in every direction. The refinement indicator threshold values for density and pressure are 0.1 kg/m^3 and 50 kPa, respectively. The CFL number in this case is set to 0.9. The 2-D simulations were performed on the high-performance computing cluster Iridis 5 at the University of Southampton, where 120 cores (Intel Xeon E5-2670 2.0 GHz) were used. The total number of four-level cells is changed dynamically from 1.6 to 2.4 M in the premixed case and is changed from 4.2 to 4.7 M in the non-premixed case instead of 12.08 M cells in the uniform case. Typical run times for the premixed and non-premixed RDE operating time 1 ms were approximately 7 to 8 days and 12 days wall-clock time, respectively.

Figure 2 shows the comparison between the premixed and non-premixed injection. In the premixed cases, a stable three-wave mode is observed. The multiple detonation waves are each followed by an oblique shock wave. Some expansion waves are observed behind the detonation wave since the premixed gases are injected discretely. In the non-premixed case, only a single detonation wave with a taller head propagates in the chamber. The average temperature is lower than that in the premixed case due

to the incomplete combustion. The results also show that the main features in the flow field, i.e., the detonation wave, the oblique shock and the mixture layer, are all captured by the finest meshes.

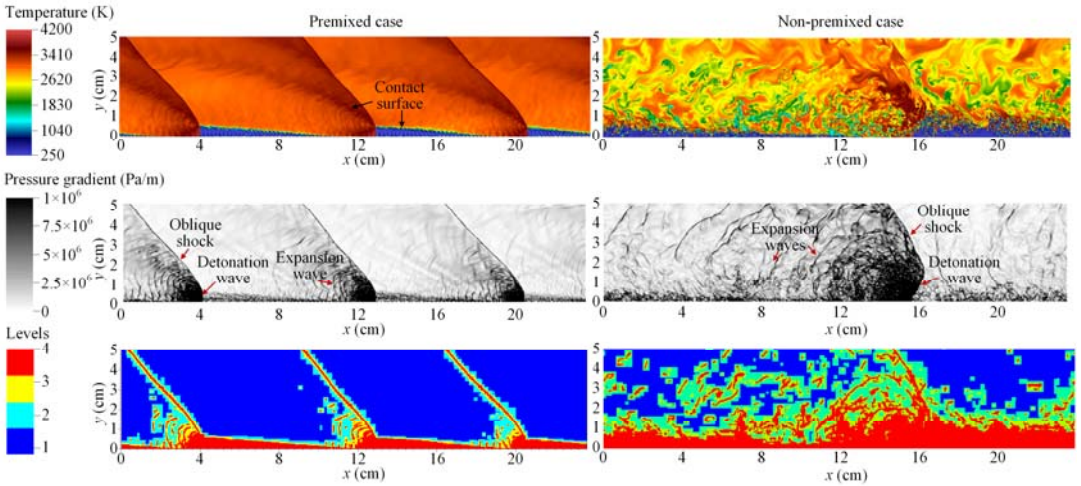

Figure 2: Pseudocolor images of temperature, pressure gradient and refinement level distribution between premixed and non-premixed RDEs.

Some probes have also been placed to monitor the pressure variations in the chamber. Figure 3 shows the pressure history of these probes from 0 ms to 1 ms simulated time and the average detonation velocity. The height of the detonation wave is estimated from Figure 2, which ranges from 4.2 mm to 5.8 mm in the premixed case and from 10 mm to 15 mm in the non-premixed case. Hence, these probes, which are 2 mm from the bottom wall, are able to measure the pressure of the detonation wave. The pressure profiles also show the difference of the number of waves.

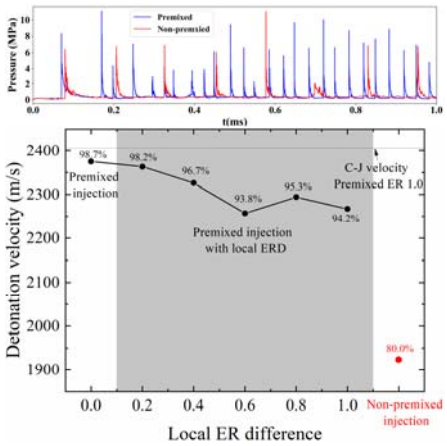

Figure 3: Pressure history in RDEs and average detonation velocity computed from the pressure profiles.

The flow velocity in the horizontal direction is computed by calculating the distance and time that the detonation wave requires to cross the probe. The average flow velocity can also be computed by calculating the interval of the cycle from the frequency of the pressure history. The average detonation velocity is computed through

the horizontal flow and vertical injection velocity, considering the inclination of the detonation wave. As depicted in Figure 3, the average propagation velocity of detonation waves declines when the local equivalence ratio differences (ERD) increase. The velocity deficit is up to 20% in the non-premixed case. For all the cases, the detonation velocity is lower than the Chapman-Jouguet (C-J) velocity of a stoichiometric mixture

.

For the 3-D case, a stoichiometric ethylene-oxygen mixture with 20% nitrogen dilution is injected from slots in the head plane. The nitrogen is considered as an inert gas. The base grid size is 0.2 mm, and a three-level refinement is used with the same factor 2 corresponding to a minimum grid size of 0.05 mm. The refinement indicator threshold value for density is 0.2 kg/m^3. The CFL number in this case is set to 0.8. The adaptive computation uses approximately 11.6 M to 12.3 M instead of 94.4 M cells in the uniform case. The calculations are performed on 480 cores (Intel Xeon E5-2670 2.0GHz). Typical run times for a simulated time of 1 ms were approximately 11 days wall clock time.

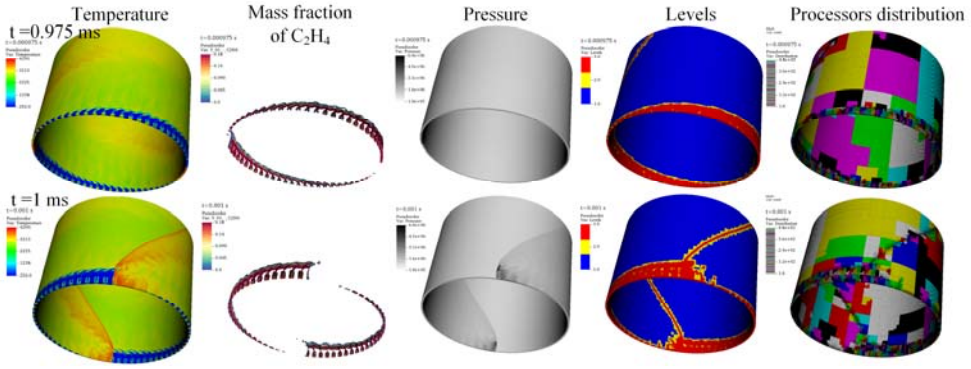

Figure 4: Pseudocolor image of temperature, isosurface of mass fraction of ethylene, pseudocolor image of pressure, refinement levels and processors distribution.

A stable two-wave mode is obtained by the 3-D simulation. Figure 4 shows that the mesh around detonation heads and in the fresh mixture layer are adaptively refined on-the-fly. More processors are used in the refined regions with higher workload. The hierarchical mesh is distributed to processors based on a space-filling curve [8] in computational space. Continuous redistribution, while the mesh is changing, is ensuring balanced workload at run time.

4 Conclusions and Contributions

The effects of a non-uniform local equivalence ratio on rotating detonation waves are studied by two-dimensional numerical simulations on parallel Cartesian adaptive meshes. Premixed and non-premixed ethylene/oxygen mixtures are injected individually. Stable multiple-wave modes are observed by the simulations. The results show the differences on the number of detonation waves in premixed and non-premixed cases. Detonation velocity deficits are also observed when increasing the local equivalence ratio difference or using a non-premixed injection.

A three-dimensional premixed RDE simulation is carried out on parallel curvilinear adaptive meshes with a recently developed solver to demonstrate its capabilities. The results confirm that the AMROC framework is effective in adapting the parallel mesh at run time to rapidly propagating localised detonation fronts.

Acknowledgements

The authors acknowledge the use of the IRIDIS High Performance Computing Facility, and associated support services at the University of Southampton. H. Peng also acknowledges financial support from China Scholarship Council (CSC).

References

[1] P. Wolański, "Detonative propulsion," Proc. Combust. Inst., vol. 34, no. 1, pp. 125–158, 2013.

[2] M. Hishida, T. Fujiwara, and P. Wolanski, "Fundamentals of rotating detonations," Shock waves, 19(1), 1-10, 2009.

[3] R. Zhou, J. P. Wang, "Numerical investigation of flow particle paths and thermodynamic performance of continuously rotating detonation engines," Combust. Flame, 159(12), 3632-3645, 2012.

[4] D. Schwer, K. Kailasanath, "Fluid dynamics of rotating detonation engines with hydrogen and hydrocarbon fuels," Proc. Combust. Inst., 34(2), 1991-1998, 2013.

[5] F. K. Lu and E. M. Braun, "Rotating detonation wave propulsion: experimental challenges, modeling, and engine concepts," J. Propuls. Power, 30(5), 1125-1142, 2014.

[6] J. Fujii, Y. Kumazawa, A. Matsuo, S. Nakagami, K. Matsuoka, and J. Kasahara, "Numerical investigation on detonation velocity in rotating detonation engine chamber," Proc. Combust. Inst., 36(2), 2665-2672, 2017.

[7] M. J. Berger and P. Colella, "Local adaptive mesh refinement for shock hydrodynamics," J. Comput. Phys., 82(1), 64-84, 1989.

[8] R. Deiterding, "Parallel adaptive simulation of multi-dimensional detonation structures," Ph.D. dissertation, Brandenburg University of Technology Cottbus, 2003.

[9] H. Peng, C. W. Atkins, and R. Deiterding, "A solver for simulating shock-induced combustion on curvilinear adaptive meshes," Comput. Fluids, 232, 105188, 2022.

[10] E. F. Toro, Riemann solvers and numerical methods for fluid dynamics: a practical introduction. Springer Science & Business Media, 2013.

[11] D. Singh and C. J. Jachimowski, "Quasiglobal reaction model for ethylene combustion," AIAA J., 32(1), 213–216, 1994.

[12] R. J. LeVeque, Finite volume methods for hyperbolic problems. Cambridge University Press, vol. 31, 2002.

[13] H. Law, T. Baxter, C. N. Ryan, and R. Deiterding, "Design and testing of a small-scale laboratory rotating detonation engine running on ethylene-oxygen," in AIAA Propulsion and Energy 2021 Forum, paper 3658, 2021.